

Channel and Radar Parameter Estimation with Fractional Delay-Doppler Using OTFS

Sai Pradeep Muppaneni, Sandesh Rao Mattu, and A. Chockalingam

Abstract—In communication systems, channel needs to be estimated at the receiver for data detection/decoding. In radar sensing, range and velocity parameters need to be estimated at the transmitter to identify and track targets/users. Waveforms and signal processing in the delay-Doppler (DD) domain are natural for the above tasks. Defined and processed in the DD domain, orthogonal time frequency space (OTFS) waveform is suited for both communication and radar sensing. In this paper, we propose an algorithm for efficient channel estimation at the receiver and range/velocity estimation at the transmitter using OTFS. The algorithm processes received pilot frames for channel estimation at the receiver and data frames echoed from the target/user for range and velocity estimation at the transmitter. A key component in the proposed algorithm is the cancellation of inter-path interference (IPI) in the DD domain. The algorithm works for fractional delay-Doppler which is a source of IPI. The proposed algorithm outperforms other channel estimation schemes and also achieves good root mean square error performance of range and velocity estimation.

Index Terms—OTFS, fractional delay-Doppler, inter-path interference, channel estimation, radar parameter estimation.

I. INTRODUCTION

Orthogonal time frequency space (OTFS) waveform has recently garnered much attention because of its suitability for both communication as well as radar sensing applications [1]–[6]. OTFS waveform is defined and processed in the delay-Doppler (DD) domain. The DD domain signal processing in OTFS modulation offers the benefit of robust communication in rapidly time-varying channels witnessed in high-mobility environments [1],[2]. OTFS waveform is also a natural waveform for radar sensing [3]–[6], where good localization attributes of the sensing waveform employed are desired to achieve increased sensing resolution/accuracy. OTFS waveform, therefore, is suited well for intelligent transportation systems where accurate joint communication and radar sensing is a key requirement [7].

In communications, accurate channel estimation is needed at the receiver for reliable data detection/decoding. Also, in radar sensing, accurate estimation of range and velocity parameters is needed at the transmitter to identify and track targets/users in the sensing environment. This paper is focused on the above two tasks using OTFS, viz., *i*) channel estimation at the receiver and *ii*) range and velocity estimation of targets/users at the transmitter by observing the received echoes from them. Specifically, we propose a novel algorithm for efficient estimation of channel at the receiver as well as range/velocity estimation at the transmitter using OTFS. At the receiver, the algorithm operates on the received pilot frame for channel estimation. At the transmitter, the same algorithm operates on the data frames echoed from the target for range and velocity

estimation. The proposed algorithm differs from the existing approaches by way of employing a scheme for canceling the DD domain inter-path interference (IPI) arising due to fractional delay-Dopplers. We term the proposed algorithm *DD inter-path interference cancellation* (DDIPIC) algorithm.

Several techniques have been proposed in the OTFS literature for channel estimation in the DD domain [8]–[14]. In [8], channel estimation is carried out using an exclusive pilot frame, assuming integer delay-Doppler values. In [9], an embedded pilot frame is considered where both data and pilot symbols are multiplexed in the same frame, with guard symbols in between. Although fractional Doppler values are considered, delays are assumed to take integer values. In [10], orthogonal matching pursuit (OMP) is used for the estimation of channel coefficients, assuming integer delay and Dopplers. A novel structure of pilot matrix is proposed in [11] to reduce pilot overhead and memory consumption. In [12], sparse Bayesian learning (SBL) algorithm is used to estimate channel coefficients, assuming integer delay and fractional Doppler values. In [13] and [14], SBL algorithm and a modified maximum likelihood estimate (M-MLE) algorithm, respectively, are used to estimate the channel with fractional delay and Dopplers. The M-MLE scheme is shown to perform better than the SBL scheme. Our DDIPIC algorithm proposed in this paper also works for fractional delay-Dopplers, and it achieves better performance compared to the M-MLE algorithm.

The use of OTFS waveform for range and velocity estimation in radar sensing applications has been studied in [3]–[6]. The works in [3],[4],[5] on OTFS for communication and sensing consider integer delay-Dopplers. Whereas, the performance of parameter estimation in these schemes are compromised when fractional delay-Dopplers are encountered (which is typical in practical channels). In [6], an iterative scheme for range and velocity estimation with fractional delay-Doppler is proposed. But this scheme assumes perfect knowledge of the number of DD domain paths in the channel. It also considers symbol detection at the receiver/target for which perfect channel knowledge is assumed. In contrast, our DDIPIC algorithm does not assume knowledge of number of DD paths at the transmitter and perfect channel knowledge at the receiver, and it achieves range and velocity estimation performance which is very close to Cramer-Rao lower bound.

II. SYSTEM MODEL

In OTFS, MN information symbols are multiplexed in the DD domain to obtain the symbol matrix $\mathbf{X}_{DD} \in \mathbb{A}^{M \times N}$ that is to be transmitted, where \mathbb{A} is the modulation alphabet from where the information symbols are drawn. M and N symbols are placed along the delay and Doppler axes, respectively, with widths T/M and $\Delta f/N$, where $\Delta f = 1/T$. The symbols in the DD domain are converted to frequency-time (FT) domain using inverse symplectic finite Fourier transform

(ISFFT), to obtain $\mathbf{X}_{\text{FT}} \in \mathbb{C}^{M \times N}$, as $\mathbf{X}_{\text{FT}} = \mathbf{F}_M \mathbf{X}_{\text{DD}} \mathbf{F}_N^H$, where \mathbf{F}_M is the unitary discrete Fourier transform (DFT) matrix of size M . \mathbf{X}_{FT} is then converted into a continuous time domain signal using the Heisenberg transform given by $x(t) = \sum_{m=0}^{M-1} \sum_{n=0}^{N-1} \mathbf{X}_{\text{FT}}[m, n] g_{\text{tx}}(t - nT) e^{j2\pi m \Delta f (t - nT)}$, where $g_{\text{tx}}(t)$ is the transmit pulse. The time domain signal $x(t)$ is passed through the channel, which is considered to have P paths in the DD domain, where the p th path has delay τ_p with $0 < \tau_p < T$ and Doppler shift ν_p . The channel is represented in the DD domain as $h(\tau, \nu) = \sum_{p=1}^P \alpha_p \delta(\tau - \tau_p) \delta(\nu - \nu_p)$, where τ_p s and ν_p s are assumed to take fractional values. This can be written in the time domain as $h(t) = \sum_{p=1}^P \alpha_p \delta(t - \tau_p) e^{j2\pi \nu_p (t - \tau_p)}$. The received signal thus becomes $y(t) = \sum_{p=1}^P \alpha_p x(t - \tau_p) e^{j2\pi \nu_p (t - \tau_p)} + w(t)$, where $w(t)$ is the additive white Gaussian noise (AWGN). The received signal is converted back to DD domain by first converting to the FT domain, using the Wigner transform to obtain $\mathbf{Y}_{\text{FT}} \in \mathbb{C}^{M \times N}$, as $\mathbf{Y}_{\text{FT}}[m', n'] = \int_t y(t) g_{\text{rx}}(t - n'T) e^{-j2\pi m' \Delta f (t - n'T)} dt$, where $m' = 0, 1, \dots, M-1$, $n' = 0, 1, \dots, N-1$, and $g_{\text{rx}}(t)$ is the receive pulse. This FT domain signal is converted to DD domain using the symplectic finite Fourier transform (SFFT), to obtain $\mathbf{Y}_{\text{DD}} \in \mathbb{C}^{M \times N}$ as $\mathbf{Y}_{\text{DD}} = \mathbf{F}_M^H \mathbf{Y}_{\text{FT}} \mathbf{F}_N$. $g_{\text{tx}}(t)$ and $g_{\text{rx}}(t)$ are assumed to be rectangular pulses of duration T and amplitude $1/\sqrt{T}$. Using the above equations, the input output relation between \mathbf{Y}_{DD} and \mathbf{X}_{DD} can be written as [14]

$$\mathbf{y}_{\text{DD}} = \sum_{p=1}^P \alpha_p \mathbf{A}_p(\tau_p, \nu_p) \mathbf{x}_{\text{DD}} + \mathbf{w}, \quad (1)$$

where $\mathbf{y}_{\text{DD}} \in \mathbb{C}^{MN \times 1}$ and $\mathbf{x}_{\text{DD}} \in \mathbb{C}^{MN \times 1}$ are vectorized forms of \mathbf{Y}_{DD} and \mathbf{X}_{DD} , respectively, i.e., $\mathbf{y}_{\text{DD}}[q'] = \mathbf{Y}_{\text{DD}}[k'M + l'] = \mathbf{Y}_{\text{DD}}[l', k']$, $\mathbf{x}_{\text{DD}}[q] = \mathbf{X}_{\text{DD}}[kM + l] = \mathbf{X}_{\text{DD}}[l, k]$, $l', l = 0, 1, \dots, M-1$, $k', k = 0, 1, \dots, N-1$, and $q', q = 0, 1, \dots, MN-1$, and \mathbf{A}_p is an $MN \times MN$ matrix whose entries are given by $\mathbf{A}_p[q', q] = e^{-j2\pi \tau_p \nu_p a a'}$, where $a = \frac{1}{N} \sum_{n=0}^{N-1} e^{-j2\pi n (\frac{k' - k}{N} - \frac{\nu_p}{\Delta f})}$, $a' = \frac{1}{M} \sum_{m=0}^{M-1} e^{j2\pi \frac{m}{M} (l' - l - M \frac{\tau_p}{T})}$, $r_{\tau_p, \nu_p, k, l'}(m)$, and $r_{\tau_p, \nu_p, k, l'}(m)$ is evaluated using (2) given at the bottom of this page.

A. Integrated communication and sensing architecture

Figure 1 shows the block diagram of the considered communication and sensing architecture. At the transmitter, two types of frames are transmitted, *i*) pilot frame (marked in yellow), and *ii*) data frame (marked in purple). The pilot frame is used at the receiver to estimate the DD channel parameters using the proposed algorithm. The estimated channel parameters are then used to detect and decode the transmitted data frames. Since the channel remains almost time-invariant in the DD domain, channel once estimated can be used for multiple data frames. This describes the communication chain from the transmitter to the receiver. Next, the symbols reflected from the receiver (referred to as target in the sensing literature) are received back at the transmitter. These frames (also called echoes), marked in blue, along with the knowledge

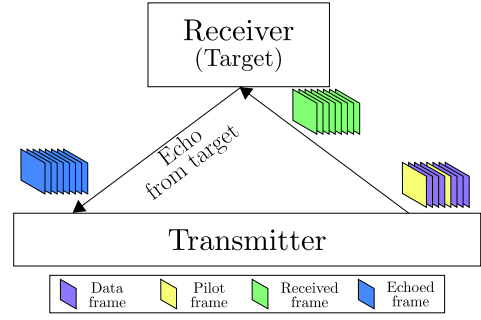


Fig. 1: Communication and sensing architecture.

of the corresponding transmitted frames are used to estimate the sensing parameters corresponding to the target, at the transmitter. The same proposed algorithm is used to estimate the sensing parameters at the transmitter. A key challenge for accurately estimating the channel and radar parameters is the inter-path interference (IPI) resulting due to the fractional DD values as explained in the following subsection.

B. Inter-path interference

Multiple copies of each transmitted symbol are received when there are P paths ($P > 1$) in the channel. For the p th path, the delay is $\tau_p = \frac{\gamma_p}{M \Delta f}$ and the Doppler is $\nu_p = \frac{\eta_p}{NT}$. In the case of integer DD, the received symbol corresponding to the p th path is localized well in the DD bin specified by the (γ_p, η_p) tuple, where $\gamma_p \in \mathbb{Z}^+$ (the set of all non-negative integers) and $\eta_p \in \mathbb{Z}$ (the set of all integers), as illustrated in Fig. 2a. On the other hand, for the fractional DD case, each transmitted symbol spreads into adjacent bins, resulting in received symbols interfering with each other (see Fig. 2b). Here, $\gamma_p \in \mathbb{R}^+$ (the set of all non-negative real numbers) and $\eta_p \in \mathbb{R}$ (the set of all real numbers). To obtain Fig. 2a, the fractional DD values used in Fig. 2b are rounded off to the nearest integer. The extent of IPI is dependent on how close or far the channel paths are in the DD grid (e.g., paths 2 and 3 in Fig. 2b exhibit higher IPI compared to other paths). IPI is a source of degradation in the channel/radar parameter estimation performance. To overcome this, we propose an algorithm that cancels the effect of IPI in a sequential manner. This enables the proposed algorithm to perform well for both the channel estimation and radar parameter estimation tasks. In the next section, we present the proposed algorithm in detail.

III. PROPOSED DDIPIC ALGORITHM

OTFS frames consisting of pilot frames interleaved among the data frames are transmitted at the transmitter (see Fig. 1). For the communication chain, the pilot frames received at the receiver are used to estimate the channel parameters, $(\hat{\alpha}_p, \hat{\tau}_p, \hat{\nu}_p)$ for $p = 1, 2, \dots, P$, which is then used to construct the effective channel matrix, $\hat{\mathbf{H}} = \sum_{p=1}^P \hat{\alpha}_p \mathbf{A}_p \in \mathbb{C}^{MN \times MN}$ (see (1)). The estimated channel matrix is used for detection of data symbols in the data frames. For the sensing chain, the reflected OTFS symbols (echoes), along

$$r_{\tau_p, \nu_p, k, l'}(m) = \sum_{s=-m}^{M-1-m} e^{j2\pi \frac{s l'}{M}} \left[\left(1 - \frac{\tau_p}{T}\right) e^{j\pi \left(1 + \frac{\tau_p}{T}\right) \left(\frac{\nu_p}{\Delta f} - s\right)} \text{sinc} \left(\left(1 - \frac{\tau_p}{T}\right) \left(\frac{\nu_p}{\Delta f} - s\right) \right) + e^{-j2\pi \frac{k}{N} \left(\frac{\tau_p}{T}\right)} e^{j\pi \left(\frac{\tau_p}{T}\right) \left(\frac{\nu_p}{\Delta f} - s\right)} \text{sinc} \left(\left(\frac{\nu_p}{\Delta f} - s\right) \right) \right]. \quad (2)$$

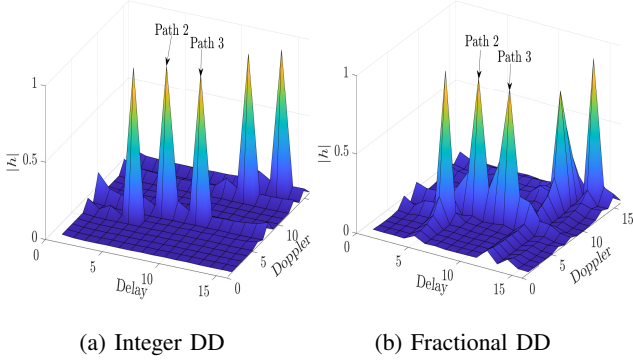


Fig. 2: Received DD domain pilot signal for integer and fractional delay-Dopplers.

with the knowledge of the transmitted OTFS symbols are used to estimate the range (d) and velocity (v) parameters of the target at the transmitter. Both these tasks are carried out using the proposed DDIPIC algorithm. The algorithm details are as follows. We can write (1) in an alternate form as

$$\mathbf{y} = \sum_{p=1}^P \mathbf{b}_p(\tau_p, \nu_p) \alpha_p + \mathbf{w} = \mathbf{B}(\boldsymbol{\tau}, \boldsymbol{\nu}) \boldsymbol{\alpha} + \mathbf{w}, \quad (3)$$

where $\mathbf{b}_p(\tau_p, \nu_p) = \mathbf{A}_p \mathbf{x}_{\text{DD}} \in \mathbb{C}^{MN \times 1}$, $\mathbf{B}(\boldsymbol{\tau}, \boldsymbol{\nu}) = [\mathbf{b}_1(\tau_1, \nu_1) \cdots \mathbf{b}_P(\tau_P, \nu_P)] \in \mathbb{C}^{MN \times P}$, $\boldsymbol{\alpha} = [\alpha_1 \cdots \alpha_P]^T \in \mathbb{C}^{P \times 1}$, and $\mathbf{w} \sim \mathcal{CN}(0, \sigma^2) \in \mathbb{C}^{MN \times 1}$. The maximum likelihood (ML) estimate of the $(\boldsymbol{\alpha}, \boldsymbol{\tau}, \boldsymbol{\nu})$ tuple can be evaluated as

$$(\hat{\boldsymbol{\alpha}}, \hat{\boldsymbol{\tau}}, \hat{\boldsymbol{\nu}}) = \underset{\boldsymbol{\alpha}, \boldsymbol{\tau}, \boldsymbol{\nu}}{\operatorname{argmin}} \|\mathbf{y} - \mathbf{B}(\boldsymbol{\tau}, \boldsymbol{\nu}) \boldsymbol{\alpha}\|^2, \quad (4)$$

which is an optimization problem with three unknowns. In order to reduce the complexity, we first estimate $\boldsymbol{\tau}$ and $\boldsymbol{\nu}$ and subsequently estimate $\boldsymbol{\alpha}$. Towards this, we note that for a given $(\boldsymbol{\tau}, \boldsymbol{\nu})$, the ML estimate of $\boldsymbol{\alpha}$ is given by

$$\hat{\boldsymbol{\alpha}} = [\mathbf{B}^H(\boldsymbol{\tau}, \boldsymbol{\nu}) \mathbf{B}(\boldsymbol{\tau}, \boldsymbol{\nu})]^{-1} \mathbf{B}^H(\boldsymbol{\tau}, \boldsymbol{\nu}) \mathbf{y}. \quad (5)$$

Representing the cost function in (4) as $(\mathbf{y} - \mathbf{B}(\boldsymbol{\tau}, \boldsymbol{\nu}) \boldsymbol{\alpha})^H (\mathbf{y} - \mathbf{B}(\boldsymbol{\tau}, \boldsymbol{\nu}) \boldsymbol{\alpha})$, simplifying, and substituting for $\boldsymbol{\alpha}$ from (5) yields the estimate as

$$[\hat{\boldsymbol{\tau}}, \hat{\boldsymbol{\nu}}] = \underset{\boldsymbol{\tau}, \boldsymbol{\nu}}{\operatorname{argmax}} [\Phi(\mathbf{B})], \quad (6)$$

where $\Phi(\mathbf{B}) = \mathbf{y}^H \mathbf{B}(\boldsymbol{\tau}, \boldsymbol{\nu}) (\mathbf{B}^H(\boldsymbol{\tau}, \boldsymbol{\nu}) \mathbf{B}(\boldsymbol{\tau}, \boldsymbol{\nu}))^{-1} \mathbf{B}^H(\boldsymbol{\tau}, \boldsymbol{\nu}) \mathbf{y}$. Using the estimates $\hat{\boldsymbol{\tau}}$ and $\hat{\boldsymbol{\nu}}$, the estimate of the channel coefficient is obtained as

$$\hat{\boldsymbol{\alpha}} = [\mathbf{B}^H(\hat{\boldsymbol{\tau}}, \hat{\boldsymbol{\nu}}) \mathbf{B}(\hat{\boldsymbol{\tau}}, \hat{\boldsymbol{\nu}})]^{-1} \mathbf{B}^H(\hat{\boldsymbol{\tau}}, \hat{\boldsymbol{\nu}}) \mathbf{y}. \quad (7)$$

To solve (6), we employ the proposed DDIPIC algorithm. Estimation of delay and Doppler values is carried out on a path by path basis. Further, this estimation is carried out in two phases, first, the coarse estimation where the search area is over integer multiples of $(\frac{1}{M\Delta f}, \frac{1}{NT})$, and second, the fine estimation where the search area is over fractional values.

The algorithm estimates a maximum of P_{\max} paths which is chosen to be more than the number of paths P in the channel. The algorithm begins by initializing $\mathbf{B}(\boldsymbol{\tau}, \boldsymbol{\nu}) = [\mathbf{b}_1(\tau_1, \nu_1) \mathbf{b}_2(\tau_2, \nu_2) \cdots \mathbf{b}_{P_{\max}}(\tau_{P_{\max}}, \nu_{P_{\max}})] = \mathbf{0}_{MN \times P_{\max}}$.

Coarse estimation: This is carried out over the search area defined by $\tau \in \{\frac{0}{M\Delta f}, \frac{1}{M\Delta f}, \dots, \frac{L}{M\Delta f}\}$ and $\nu \in$

Algorithm 1 Fine estimation of channel parameters

- 1: **Inputs:** Coarse estimates, (τ'_p, ν'_p) , refinements, m_τ, n_ν , and convergence indicators $\epsilon_\tau, \epsilon_\nu$
 - 2: **Initialize:** Counter, $s = 1$, $\hat{\tau}^{(1)} = \tau'_p$, and $\hat{\nu}^{(1)} = \nu'_p$
 - 3: **repeat**
 - 4: search width in delay, $w_\tau^{(s)} = \frac{1}{M\Delta f m_\tau^{s-1}}$
 - 5: search width in Doppler, $w_\nu^{(s)} = \frac{1}{NT n_\nu^{s-1}}$
 - 6: $\mathbf{F}^{(s)} = \{w_\tau^{(s)} \gamma + \hat{\tau}^{(s)}\} \otimes \{w_\nu^{(s)} \chi + \hat{\nu}^{(s)}\}$, search area for fractional DD
 - 7: $\hat{\tau}^{(s+1)}, \hat{\nu}^{(s+1)} = \underset{(\tau, \nu) \in \mathbf{F}^{(s)}}{\operatorname{argmax}} \Phi(\mathbf{B})$
 - 8: **update** $s = s + 1$
 - 9: **until** $s = S_{\max}$ or $(|\hat{\tau}^{(s+1)} - \hat{\tau}^{(s)}| < \epsilon_\tau$ and $|\hat{\nu}^{(s+1)} - \hat{\nu}^{(s)}| < \epsilon_\nu)$
 - 10: **Output:** $\hat{\tau}_p = \hat{\tau}^{(s+1)}$ and $\hat{\nu}_p = \hat{\nu}^{(s+1)}$
-

$\{-\frac{K}{NT}, \dots, \frac{0}{NT}, \dots, \frac{K}{NT}\}$. For estimating the first path, $\mathbf{b}_1(\tau_1, \nu_1)$ is evaluated with (τ_1, ν_1) taking all possible combinations of (τ, ν) in the search area. To choose the optimal coarse value of the estimate, (τ'_1, ν'_1) , we maximize the cost function $\Phi(\mathbf{B})$ in (6).

Fine estimation: This is carried out in a search area around the optimal coarse value obtained in the previous step. Fine estimation of the parameters is carried out iteratively, where the search area is narrowed down as the iterations progress. This iterative procedure is presented in **Algorithm 1**, where $\gamma = \{-\lfloor \frac{m_\tau}{2} \rfloor, \dots, 0, \dots, \lfloor \frac{m_\tau}{2} \rfloor\}$, $\chi = \{-\lfloor \frac{n_\nu}{2} \rfloor, \dots, 0, \dots, \lfloor \frac{n_\nu}{2} \rfloor\}$, and the operator \otimes denotes the Cartesian product of two sets. At the end of the iterations, the fine estimates $\hat{\tau}_1$ and $\hat{\nu}_1$ are obtained for the first path.

For the estimation of parameters of the t th path, columns $1, 2, \dots, t-1$ in \mathbf{B} are filled using $(\hat{\tau}_p, \hat{\nu}_p)$ s obtained after fine estimation. Coarse estimates for τ_t and ν_t are obtained by maximizing the cost function in (6) over different values of (τ, ν) (as defined in the coarse estimation stage) in the t th column of \mathbf{B} . This is followed by fine estimation using **Algorithm 1**.

Stopping criterion: At the end of fine estimation for t th path, the matrix $\mathbf{B}(\hat{\boldsymbol{\tau}}, \hat{\boldsymbol{\nu}})$ is obtained. Further, $\hat{\boldsymbol{\alpha}}$ is obtained using (7). A residue vector, $\mathcal{E}^{(t)}$ is obtained as $\mathcal{E}^{(t)} = \mathbf{y} - \mathbf{B}(\hat{\boldsymbol{\tau}}, \hat{\boldsymbol{\nu}}) \hat{\boldsymbol{\alpha}}$. The algorithm stops at t paths if $\|\mathcal{E}^{(t)} - \mathcal{E}^{(t-1)}\|^2 < \epsilon$, which is the stopping criterion. If this criterion is not met until $t = P_{\max}$, the algorithm is stopped when the number of estimated paths reaches P_{\max} .

Refinement of parameter estimates: After the estimation of t th path, $1 < t < P_{\max}$, if the stopping criterion is not met, we refine the previously obtained estimates before estimating the parameters of the $(t+1)$ th path. This refinement proceeds as follows. For the z th path, with $1 \leq z \leq t$, we use the estimates $(\hat{\tau}_i, \hat{\nu}_i)$ s with $i = 1, 2, \dots, z-1, z+1, \dots, t$, to obtain the matrix \mathbf{B} (i.e., fill all the columns in \mathbf{B} except the z th column). We then evaluate the refined estimates of the z th path again, by optimizing the cost function in (6) for the z th column of \mathbf{B} . This is carried out first over the coarse search area and then over the fine search area. Following this, the estimate of parameters of the $(t+1)$ th path is obtained using the refined estimates of all the paths till t . This is illustrated

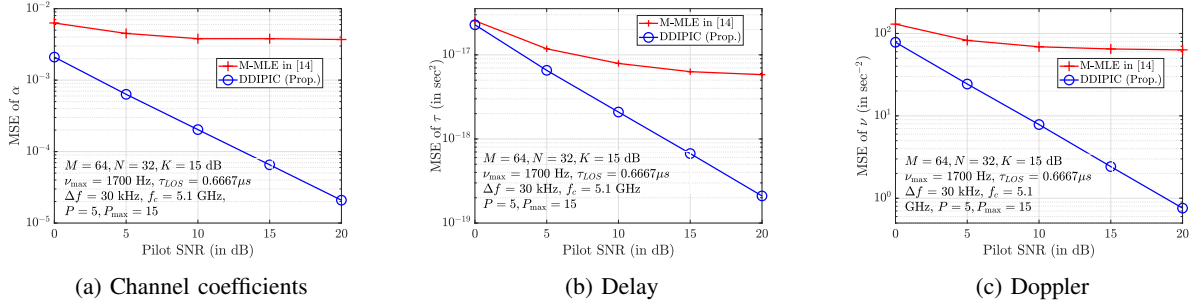


Fig. 3: MSE of estimated parameters as a function of pilot SNR.

Operation	Complex multiplications	Complex additions	Total complexity
$\Xi = \mathbf{Y}^H \mathbf{B}(\tau, \nu)$	$P_{\max} MN$	$P_{\max}(MN - 1)$	$2P_{\max} MN - P_{\max}$
$\mathbf{Y} = \mathbf{B}^H(\tau, \nu) \mathbf{B}(\tau, \nu)$	$P_{\max}^2 MN$	$P_{\max}^2(MN - 1)$	$2P_{\max}^2 MN - P_{\max}^2$
\mathbf{Y}^{-1}			$\mathcal{O}(P_{\max}^3)$
$\Xi \mathbf{Y}^{-1}$	P_{\max}^2	$P_{\max}(P_{\max} - 1)$	$2P_{\max}^2 - P_{\max}$
$\Xi \mathbf{Y}^{-1} \Xi^H$	P_{\max}	$P_{\max} - 1$	$2P_{\max} - 1$

TABLE I: Computational complexity for cost function.

Estimation stage	Complexity (value $\times C$)
Coarse estimation	$C' = (L + 1)(2K + 1)P_{\max}$
Fine estimation	$C'' = (2\lceil \frac{m_\tau}{2} \rceil + 1)(2\lceil \frac{n_\nu}{2} \rceil + 1)P_{\max}$
Refinement	$\left(\frac{(P_{\max} - 1)P_{\max}}{2} - 1 \right) (C' + C'')$
Channel coefficient	1

TABLE II: Complexity in different stages of estimation.

with the following example. When $t = 3$, three paths are estimated, and the stopping criterion is not met, then

- 1st path is refined using the 2nd and 3rd paths (both unrefined),
- 2nd path is refined using the refined first path and the 3rd path (unrefined), and
- 3rd path is refined using the refined 1st and 2nd paths.

The estimate of the parameters of the 4th path is obtained using the refined 1st, 2nd, and 3rd path estimates.

Remark on IPI cancellation: Initial unrefined estimates are obtained in the presence of interference from other paths (see Fig. 2b). To handle IPI and to combat its effect, we refine the parameter estimates as described above. In the above example, when the refined estimate is obtained for the first path, the effect of interference from second and third paths is reduced, which was present in the unrefined estimate for the first path. In effect, the refinement procedure followed above results in IPI cancellation that helps the DDIPIIC algorithm achieve better mean square error performance as will be shown in the performance results section (Sec. IV).

Complexity: Table I shows the computation complexity of the proposed estimator (6) in terms of number of complex additions and multiplications. The sum of the last column, $C = 2P_{\max} MN + 2P_{\max}^2 MN + P_{\max}^2 + \mathcal{O}(P_{\max}^3) - 1$ is the total number of operations required to compute (6). Table II shows the maximum number of times the cost function in (6) is evaluated in each stage of estimation. The sum of the last column multiplied with C denotes the maximum complexity of the proposed algorithm.

IV. RESULTS AND DISCUSSIONS

In this section, we present the numerical results on the performance of the proposed DDIPIIC algorithm. We consider $M = 64$, $N = 32$, $\Delta f = 30$ kHz, and $f_c = 5.1$ GHz. The channel is assumed to have $P = 5$ resolved paths with a line of sight (LOS) path and a Rice factor (K) of

15 dB [14]. The delay of the first and second paths are taken to be $0.667 \mu\text{s}$, $0.867 \mu\text{s}$, respectively, and the delays of other paths are uniformly distributed in $(0.867 \mu\text{s}, 7 \mu\text{s})$. Doppler frequencies for all the paths are generated from Jake's Doppler spectrum using $\nu_p = \nu_{\max} \cos(\theta_p)$ where θ_p is uniformly distributed in $(0, 2\pi]$ and ν_{\max} is 1700 Hz. The fixed absolute squared value of the channel gain of LOS path is taken according to the Rice factor, and exponential power delay profile is used for the other paths as in [14]. Further, $m_\tau = n_\nu = 10$, $\epsilon_\tau = 10^{-10}$, $\epsilon_\nu = 10^{-2}$, and $\epsilon = 0.01NM\sigma^2$, where σ^2 is the noise variance.

A. Channel estimation performance at receiver

1) **MSE performance of channel parameters:** Figure 3 shows the MSE performance of the channel parameters obtained using the proposed DDIPIIC algorithm for the LOS path. Specifically, MSE of the channel coefficient, delay, and Doppler values are presented in Figs. 3a, 3b, and 3c, respectively. The MSE performance of the channel parameters obtained using the M-MLE algorithm is also presented for comparison. It is seen that for all the channel parameters, the MSE performance using the proposed DDIPIIC is observed to decrease almost linearly with pilot SNR. On the other hand, the MSE performance of M-MLE algorithm is seen to floor.

2) **NMSE performance:** Normalized mean square error (NMSE) is evaluated as $\mathbb{E} \left[\frac{\|\mathbf{H} - \hat{\mathbf{H}}\|_F^2}{\|\mathbf{H}\|_F^2} \right]$. Figure 4 shows the NMSE performance of the channel matrix obtained using the proposed DDIPIIC algorithm. The NMSE performance obtained using the M-MLE algorithm in [14] is also presented for comparison. It is seen that the NMSE performance of both the schemes decrease almost linearly with pilot SNR. However, the NMSE performance with the proposed DDIPIIC is better when compared to that of the M-MLE scheme. For example, NMSE value of -30 dB is obtained at around 10 dB of pilot SNR with the proposed scheme, as opposed to 15 dB with the M-MLE scheme.

3) **BER performance:** Figure 5 shows the BER performance of the proposed DDIPIIC algorithm for a pilot SNR of 10 dB. BER performance with perfect CSI is also added for reference along with the performance of M-MLE scheme. Minimum mean square error (MMSE) detection is used and the data symbols are drawn from 64-QAM modulation alphabet. First, it is observed that the proposed DDIPIIC algorithm achieves better performance compared to the M-MLE scheme. For example, a BER of 10^{-3} is achieved at 24 dB for the proposed scheme, while it is achieved at about 28 dB for the M-MLE scheme. This performance gain is attributed to the refinement

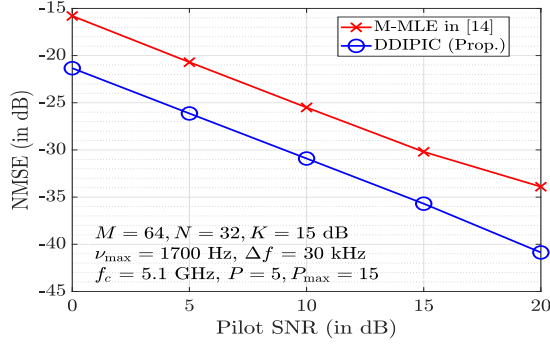


Fig. 4: NMSE performance of the proposed DDIPIC algorithm as a function of pilot SNR.

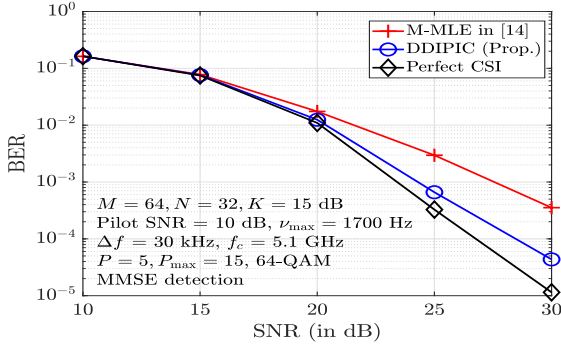


Fig. 5: BER performance of the proposed DDIPIC algorithm as a function of SNR.

of parameter estimates achieved through IPI cancellation in the proposed algorithm. Further, the proposed algorithm is observed to perform close to that with perfect CSI.

B. Radar parameter estimation performance at transmitter

In this subsection, we present range and velocity estimation performance of the proposed algorithm, with $M = 64$, $N = 50$, $f_c = 5.89$ GHz, and $\Delta f = 156.25$ kHz. The range and velocity of the target are considered to be 20 m and 80 km/h, respectively. The above parameters are as in [6]. Figure 6 shows the root mean square error (RMSE) performance of range estimation as a function of SNR achieved with the proposed DDIPIC algorithm. The performance achieved with the scheme in [6] is also shown for comparison. Further, the Cramer-Rao lower bound (CRLB) for the considered system is also plotted. It is seen that the proposed scheme and the scheme in [6] perform similarly and this performance is close to the CRLB. Figure 7 shows the RMSE performance of velocity estimation as a function of SNR for the proposed algorithm and the scheme in [6] along with the CRLB. Similar to the delay estimation performance, both the approaches exhibit similar velocity estimation performance that is close to CRLB. However, we note that the scheme in [6] assumes the knowledge of the number of paths, whereas the proposed DDIPIC algorithm requires no such knowledge.

REFERENCES

[1] R. Hadani et al., "Orthogonal time frequency space modulation," *Proc. IEEE WCNC 2017*, pp. 1-6, Mar. 2017.
[2] Z. Wei et al., "Orthogonal time-frequency space modulation: a promising next-generation waveform," *IEEE Wireless Commun. Mag.*, vol. 28, no. 4, pp. 136-144, Aug. 2021.

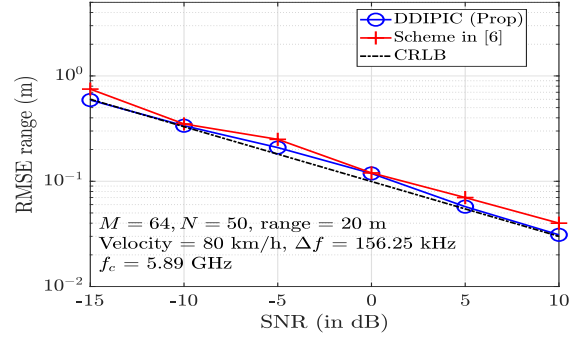


Fig. 6: RMSE of range as a function of SNR achieved with the proposed DDIPIC algorithm and the scheme in [6].

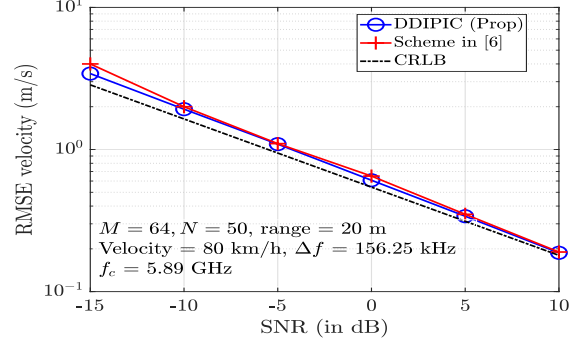


Fig. 7: RMSE of velocity as a function of SNR achieved with the proposed DDIPIC algorithm and the scheme in [6].

[3] W. Yuan, Z. Wei, S. Li, J. Yuan, and D. W. K. Ng, "Integrated sensing and communication-assisted orthogonal time frequency space transmission for vehicular networks," *IEEE J. Sel. Topics in Signal Process.*, vol. 15, no. 6, pp. 1515-1528, Dec. 2021.
[4] P. Raviteja, K. T. Phan, Y. Hong, and E. Viterbo, "Orthogonal time frequency space (OTFS) modulation based radar system," *Proc. IEEE Radar Conf.*, pp. 1-6, Apr. 2019.
[5] S. Li, W. Yuan, C. Liu, Z. Wei, J. Yuan, B. Bai, and D. W. K. Ng, "A novel ISAC transmission framework based on spatially-spread orthogonal time frequency space modulation," *IEEE J. Sel. Areas Commun.*, vol. 40, no. 6, pp. 1854-1872, Jun. 2022.
[6] L. Gaudio, M. Kobayashi, G. Caire, and G. Colavolpe, "On the effectiveness of OTFS for joint radar parameter estimation and communication," *IEEE Trans. Wireless Commun.*, vol. 19, no. 9, pp. 5951-5965, Sep. 2020.
[7] D. Ma, N. Shlezinger, T. Huang, Y. Liu, and Y. C. Eldar, "Joint radar communications strategies for autonomous vehicles: combining two key automotive technologies," *IEEE Signal Process. Mag.*, vol. 37, no. 4, pp. 85-97, Jul. 2020.
[8] M. K. Ramachandran and A. Chockalingam, "MIMO-OTFS in high-Doppler fading channels: signal detection and channel estimation," *Proc. IEEE GLOBECOM 2018*, pp. 206-212, Dec. 2018.
[9] P. Raviteja, K. T. Phan, Y. Hong, and E. Viterbo, "Embedded pilot-aided channel estimation for OTFS in delay-Doppler channels," *IEEE Trans. Veh. Tech.*, vol. 68, no. 5, pp. 4906-4917, May 2019.
[10] W. Shen, L. Dai, J. An, P. Fan, and R. W. Heath, "Channel estimation for orthogonal time frequency space (OTFS) massive MIMO," *IEEE Trans. Signal Process.*, vol. 67, no. 16, pp. 4204-4217, Aug. 2019.
[11] D. Shi, W. Wang, L. You, X. Song, Y. Hong, X. Gao and G. Fettweis, "Deterministic pilot design and channel estimation for downlink massive MIMO-OTFS systems in presence of the fractional Doppler," *IEEE Trans. Wireless Commun.*, vol. 20, no. 11, pp. 7151-7165, Nov. 2021.
[12] F. Liu, Z. Yuan, Q. Guo, Z. Wang, and P. Sun, "Message passing based structured sparse signal recovery for estimation of OTFS channels with fractional Doppler shifts," *IEEE Trans. Wireless Commun.*, vol. 20, no. 12, pp. 7773-7785, Dec. 2021.
[13] Z. Wei, W. Yuan, S. Li, J. Yuan, D. W. K. Ng, "Off-grid channel estimation with sparse Bayesian learning for OTFS systems," *IEEE Trans. Wireless Commun.*, vol. 21, no. 9, pp. 7407-7426, Sep. 2022.
[14] I. A. Khan and S. K. Mohammed, "Low complexity channel estimation for OTFS modulation with fractional delay and Doppler," arXiv:2111.06009 [cs.IT] 11 Nov 2021.